Apoptosis-like, reversible changes in plasma membrane asymmetry and permeability, and transient modifications in mitochondrial membrane potential induced by curcumin in rat thymocytes

Ewa Jaruga[a,*], Stefano Salvioli[b], Jurek Dobrucki[c], Sławomir Chrul[d], Joanna Bandorowicz-Pikuła[e], Ewa Sikora[e], Claudio Franceschi[b,f], Andrea Cossarizza[b], Grzegorz Bartosz[a]

[a]*Department of Molecular Biophysics, University of Lodz, Banacha 12/16, 90-237 Lodz, Poland*
[b]*Department of Biomedical Sciences, University of Modena School of Medicine, Modena, Italy*
[c]*Laboratory of Confocal Microscopy and Image Analysis, Department of Biophysics, Jagiellonian University, Cracow, Poland*
[d]*Laboratory of Flow Cytometry, Medical University of Lodz, Lodz, Poland*
[e]*Nencki Institute of Experimental Biology, Warsaw, Poland*
[f]*Department of Gerontological Sciences, INRCA, Ancona, Italy*

Received 19 June 1998

Abstract Curcumin (diferuoylmethane) is a natural compound with anticarcinogenic activities which is able to exert either proapoptotic or antiapoptotic effects in different cell types. This paper focuses on the sequence and extent of primary events induced by curcumin, in comparison with those occurring during dexamethasone-induced apoptosis in rat thymocytes. It also presents annexin VI-FITC as a new probe for studying membrane asymmetry. Curcumin readily penetrates into the cytoplasm, and is able to accumulate in membranous structures such as plasma membrane, endoplasmic reticulum and nuclear envelope. Curcumin-treated cells exhibit typical features of apoptotic cell death, including shrinkage, transient phosphatidylserine exposure, increased membrane permeability and decrease in mitochondrial membrane potential. However, nuclei morphology, DNA fragmentation, the extent and time-course of membrane changes are different from those observed during dexamethasone-induced apoptosis, suggesting that, despite many similarities, the mode of action and the events triggered by curcumin are different from those occurring during typical apoptosis.

Key words: Apoptosis; Curcumin; Membrane asymmetry; Permeability; Mitochondrial membrane potential

1. Introduction

Growing interest focuses on new antitumor strategies which involve the regulation of the cell death program [1]. Curcumin (CUR, 1,7-bis(4-hydroxy-3-methoxyphenyl)-1,6-heptadiene-3,5-dione), the natural yellow dye from powdered rhizomes of *Curcuma* species, exhibits antiinflammatory, antimutagenic and anticarcinogenic activities [2,3]. CUR inhibits cell proliferation and can affect cell cycle [4,5]. Interestingly, it has been reported that CUR exerts opposite effects on apoptosis, showing either stimulation of this phenomenon in proliferating promyelocytic leukemia HL-60 cells [6], or its prevention in dexamethasone-treated rat thymocytes [5]. To explain this paradox, a broad spectrum of mechanisms have been proposed which include alterations in arachidonate metabolism [7,8], inhibition of protein kinase C [9], and redox regulation [10,11].

In this paper, we analyzed the primary effects of the presence of CUR in rat thymocytes, and compared the sequence and extent of CUR-evoked events with those occurring during the typical apoptotic program induced by dexamethasone (DEX). The fluorescence and lipophilic properties of CUR [12] provided the basis for the search of its cellular localization and for analyzing the local effects on the structure and function of cellular membranes. Plasma membrane asymmetry was studied by a new fluorescence probe, i.e. annexin VI (Anx VI), isolated from porcine liver and coupled with FITC. We could investigate other parameters such as plasma membrane permeability, mitochondrial membrane potential, as well as other typical apoptotic features ,i.e. changes in cell volume, nucleus morphology and DNA fragmentation.

2. Materials and methods

2.1. Cell cultures and drug exposure

Thymocytes were isolated from 3–4 week old rats of a WKY/Ola/Hsd/Lod barrier reared, inbred strain, as previously described [13]. Cells (5×10^6/ml) were incubated in RPMI 1640 medium supplemented with 10% fetal calf serum, 100 IU penicillin, 100 μg/ml streptomycin, 2 mM L-glutamine in a humidified atmosphere of 5% CO_2 in air at 37°C. 50 μM CUR (Sigma; 10 mM stock in methanol, protected from light, stored at −20°C) was used in the presence or absence of 10^{-7} M DEX (Sigma)

2.2. Analysis of cell membrane asymmetry and permeability

2.2.1. Purification of annexin VI from porcine liver and FITC-Anx VI preparation. The fraction of Ca^{2+}-precipitable proteins from porcine liver homogenate was purified according to [14] and stored at 1–2 mg/ml in 20 mM Tris-HCl, pH 7.4, 1 mM EGTA at −20°C. The purity of Anx VI was analyzed by SDS-PAGE. FITC (fluorescein isothiocyanate isomer I, Sigma) coupling to Anx VI was performed as described [15]. Briefly, after dialysis against a FITC coupling buffer (50 mM sodium borate-NaOH, pH 9.0, 150 μM NaCl, 1 mM EDTA) Anx VI was mixed with FITC (1:2, mol/mol) and incubated for 2 h at 37°C. The reaction was stopped by the addition of 100 mM glycine and the mixture was dialyzed against 50 mM Tris-HCl, pH 8.0, 80 mM NaCl, 1 mM EDTA. The complex was purified using FPLC (Pharmacia) system with MonoQ column (NaCl gradient: 80–400

*Corresponding author. Fax: (48) (42) 6354473.
E-mail: karla@biol.uni.lodz.pl

Abbreviations: CUR, curcumin; CON, control, non-treated; DEX, dexamethasone; FITC, fluorescein isothiocyanate; FSC, forward scatter; SSC, side scatter; Anx VI, annexin VI; JC-1, 5,5′,6,6′-tetrachloro-1,1′,3,3′-tetraethylbenzimidazolcarbocyanine iodide; PI, propidium iodide; PS, phosphatidylserine; $\Delta\psi_m$, mitochondrial membrane potential

PII: S0014-5793(98)00919-3

mM at 1 ml/min) and analyzed for protein content and at 492 nm (FITC content, $\varepsilon = 78\,000$ mol^{-1} l cm^{-1}).

2.2.2. Double staining with FITC-Anx VI+propidium iodide (PI). Annexins preferentially bind to negatively charged phospholipids such as phosphatidylserine (PS) [15]. We used a two-color flow cytometric approach with FITC-Anx VI/PI, which allows the identification of three cell subpopulations on the FL-1/FL-2 dot plot: PS^-/PI^- (intact cells), PS^+/PI^- (cells with lost asymmetry but preserved membrane integrity) and PS^+/PI^+ (cells with compromised membrane). One million cells were washed with PBS and resuspended in binding buffer (10 mM HEPES-NaOH, pH 7.4, 140 NaCl, 2.5 mM $CaCl_2$). FITC-Anx VI was added at a final concentration of 1 μg/ml, and PI was simultaneously added (see below). After 10 min incubation in the dark at room temperature, cells were analyzed by flow cytometry. Considering that the natural fluorescence of CUR can slightly interfere with the emission of FITC and PI, we set control gates on the FL-1/FL-2 dot plot for CUR-treated and non-treated cells before labelling with FITC-Anx VI or PI. However, the amount of unspecific staining due to the natural fluorescence of CUR was always $< 2\%$ (data not shown). Cell volume changes were monitored concomitantly by analysis of forward scatter (FSC), considering the ability of the cells to exclude PI and expose PS.

2.2.3. PI exclusion test. Short incubation with PI, a charged cationic dye (Sigma), results in selective labelling of cells with a defective transport system and lost structural integrity [16]. The assay distinguishes on the FSC/FL-2 dot plot early apoptotic cells (PI^{dim}) and late apoptotic/necrotic (PI^{bright}) from control cells (PI^-) independently of DNA oligonucleosomal fragmentation. 2.5×10^5 cells were washed and suspended in PBS. Thymocytes were stained supravitally with 5 μg/ml PI in PBS for 10 min in the dark at room temperature and subsequently analyzed by FACS.

2.3. Measurement of mitochondrial membrane potential $\Delta\psi_m$

$\Delta\psi_m$ was measured by using the specific, fluorescent lipophilic cation JC-1 (5,5′,6,6′-tetrachloro-1,1′,3,3′-tetraethylbenzimidazolcarbocyanine iodide, from Molecular Probes, Eugene, OR), as described [17–21]. JC-1 exists in monomeric form ($\lambda_{ex} = 490$ nm; $\lambda_{em} = 527$ nm), selectively enters into mitochondria and in the presence of a high $\Delta\psi_m$ reversibly forms aggregates ($\lambda_{em} = 590$ nm). Both the λ_{em} can be evaluated by most flow cytometers at the FL-1/FL-2 dot plot. Additional, control samples were always prepared treating cells with 100 nM valinomycin, capable of collapsing $\Delta\psi_m$, to test the decrease in JC-1 red fluorescence, as already reported [17]. The fluorescence of curcumin ($\lambda_{abs} = 420$ nm; $\lambda_{em} = 495$) did not interfere with the detection of JC-1 monomers or aggregates (data not shown). 2.5×10^5 thymocytes were incubated with 2.5 μg/ml JC-1 in the dark for 10 min at room temperature in complete medium. Then, cells were washed twice in PBS, resuspended in 400 μl PBS and analyzed by flow cytometry.

2.4. Analysis of hypodiploid nuclei

DNA content was analyzed in the nuclei by reduced fluorescence of the classical DNA binding dye PI according to Nicoletti et al. [22]. Briefly, 1×10^6 cells were washed in PBS and gently resuspended in 1 ml of 50 μg/ml PI in hypotonic solution (0.1% sodium citrate, 0.1% Triton X-100, Sigma) and incubated for at least 30 min prior to FACS measurement. The subdiploid DNA peak of apoptotic nuclei can be discriminated from the narrow peak of diploid DNA content on the red fluorescence histogram. Changes in forward and side scatter properties (FSC/SSC) were also analyzed.

2.5. Confocal microscopy studies

Thymocytes (5×10^6/ml) were suspended in cold DMEM without phenol red and bicarbonate (Sigma) supplemented with 1.25% meth-

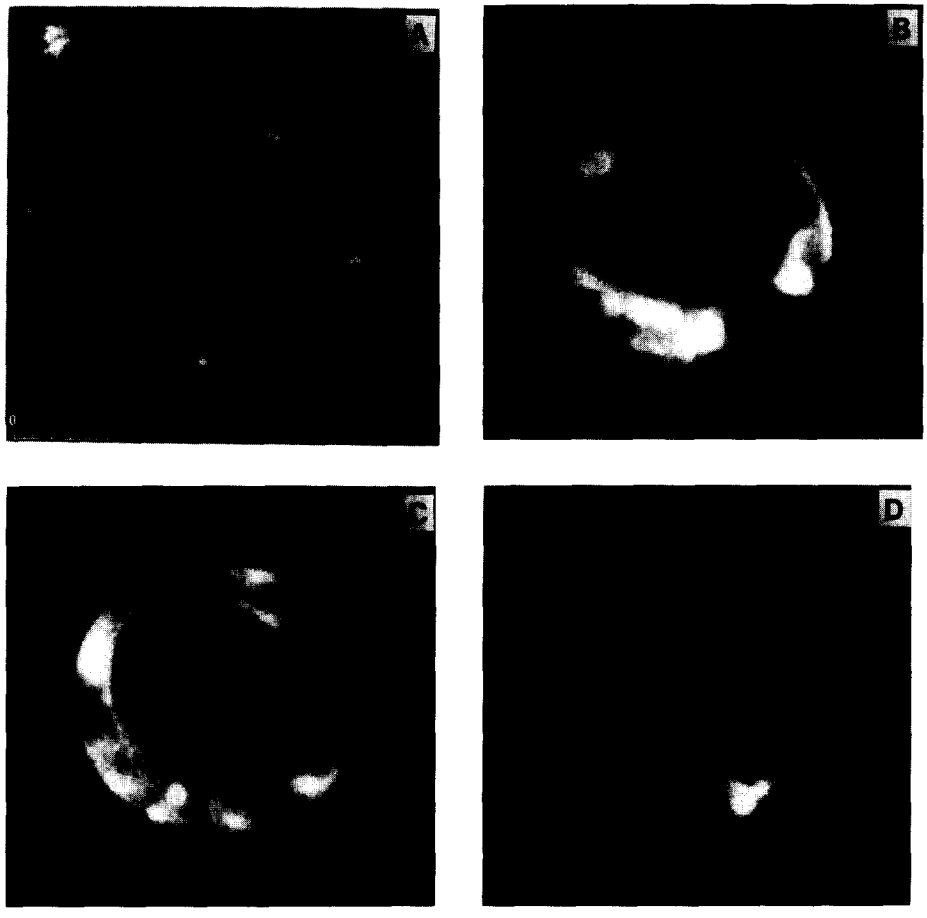

Fig. 1. Accumulation of curcumin in rat thymocytes. A: Typical image of curcumin-stained thymocytes 5 min following addition of the drug. B and C: An optical slice through the cell center – staining is present exclusively in the cytoplasm. Nucleus is not stained. D: An optical slice collected in an area of the thick layer of cytoplasm adjacent to the nucleus.

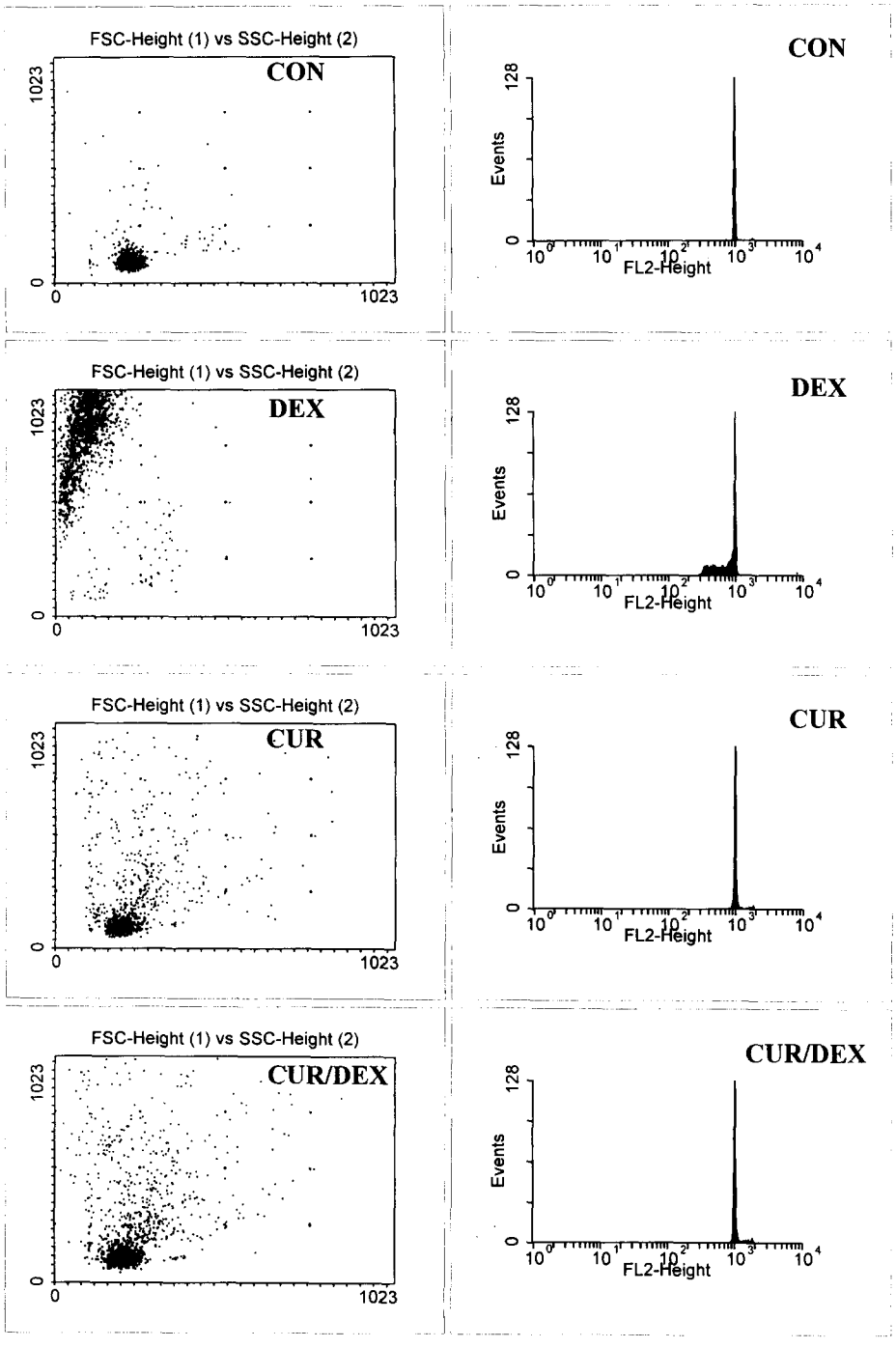

Fig. 2. Changes in nuclear morphology and DNA content in rat thymocytes incubated for 20 h with curcumin (50 μM; CUR) and/or dexamethasone (10^{-7} M; DEX); CON, control, non-treated cells. A: Changes in physical parameters (FSC and SSC) of nuclei. B: Sub-G_1 fraction in thymocyte nuclei. Data are representative of three experiments.

ylcellulose (Sigma). pH was adjusted to 7.4 using HEPES. Curcumin was added to a final concentration of 50 μM and the cell suspension was placed in a microincubator (Life Science Resources, Cambridge). Cells were maintained on a microscope stage at 37°C throughout the experiment. Images of curcumin fluorescence were recorded using a Bio-Rad MRC1024 confocal microscope, equipped with a 100 mW Ar ion laser (ITL). The 457 nm line was used for excitation, fluorescence was collected in the region of 540 ± 15 nm. Integrity of plasma membranes was tested by exclusion of PI (5 μg/ml in PBS). Green and red autofluorescence of thymocytes was negligible under the conditions of the experiment.

2.6. Statistical analysis

The data are presented as the means ± S.D. of at least three separate experiments. The differences between means after the indicated treatments were analyzed using Fisher test (variance analysis). Significances of differences were calculated using Student's *t*-test. Means were considered significantly different at $P < 0.05$.

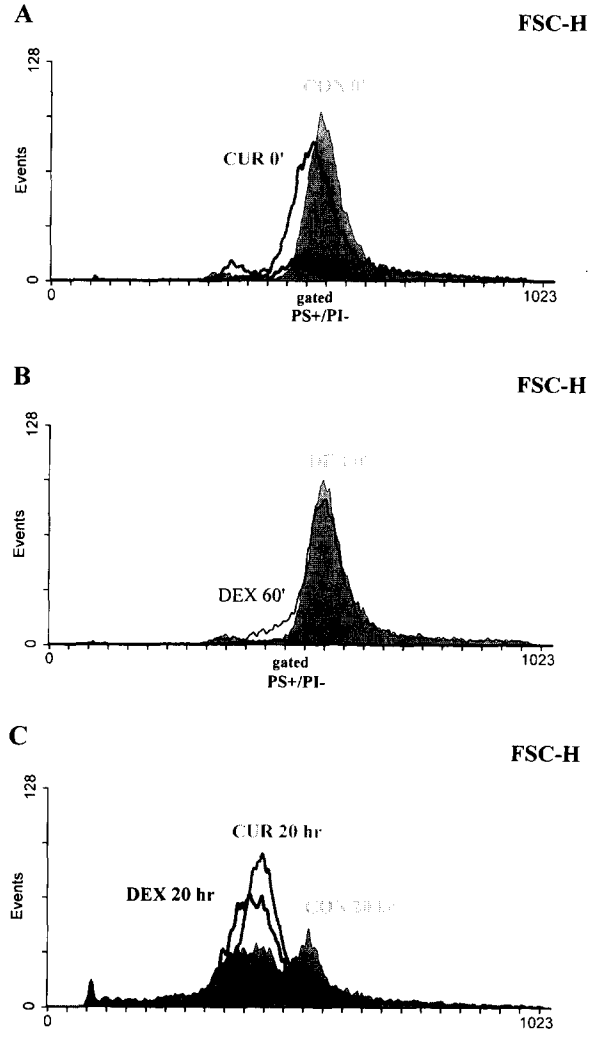

Fig. 3. Changes in FSC of thymocytes during 20 h of incubation with indicated additives. A: Immediate shrinkage of CUR-treated cells (50 μM, CUR 0 h, gray line), compared with non-treated cells (CON 0 h, shaded). Gated PS^+/PI^- cells (black line) after CUR addition are smaller than non-treated cells. B: Peak broadening of DEX-stimulated cells after 1 h (10^{-7} M, DEX 1 h, thin line), compared with DEX-treated cells at time 0 h (DEX 0 h, shaded). Gated PS^+/PI^- cells (black line) after 1 h of DEX stimulation are smaller than non-treated cells. C: Cell shrinkage after 20 h incubation with 50 μM CUR coadministrated with 10^{-7} M DEX (CUR/DEX 20 h, gray line) did not differ from apoptotic shrinkage (DEX 20 h, black line). CON 20 h (non-treated cells, shaded). Data are representative of three experiments.

3. Results

3.1. Subcellular localization of curcumin

Confocal images of thymocytes incubated in the presence of curcumin revealed a rapid penetration of the drug into intact cells. Curcumin did not enter cell nuclei and appeared to accumulate in a cytoplasmic compartment. Probably due to its lipophilic characteristics, the drug seemed to partition exclusively into membranous structures such as plasma membrane, endoplasmic reticulum and nuclear envelope (Fig. 1). Staining of intracellular structures was seen in the cells with intact plasma membranes (i.e. those excluding PI). Curcumin did not enter cell nuclei even in cells whose plasma membrane integrity was compromised (as demonstrated by their permeability to PI). This observation would suggest that curcumin is able to spread through the lipid phase of membranous structures inducing local changes there.

3.2. Nucleus morphology and DNA content

Exposure to CUR resulted in the appearance of nuclei with higher FSC and SSC compared to controls. The number of morphologically different nuclei increased with time, from 6 to 20 h of incubation, regardless of DEX presence. However, the majority of nuclei preserved the same FSC/SSC properties of control samples (Fig. 2A, CUR; CUR/DEX). No cells treated with CUR (CUR alone or CUR plus DEX) showed hypodiploid characteristic, while about 3/4 of DEX-stimulated thymocytes presented changes typical of apoptotic cells (Fig. 2B, CUR and CUR/DEX vs. DEX). As expected, in almost all nuclei DEX caused a decrease of FSC and an increase of SSC (Fig. 2A, DEX) due to nucleus fragmentation and chromatin condensation, respectively.

3.3. Cell volume changes

Curcumin induced an immediate shrinkage of the cell population, as was presented on a FSC histogram by a shift of the main peak to the left, comparing to non-treated cells (Fig. 3A, CUR 0 vs. CON). DEX coadministration did not significantly change this picture (not shown). CUR-treated cells with exposed PS (PI^-PS^+) were a part of the shifted main peak while the cells with compromised plasma membrane (PI^+) represented a distant peak of smaller cells, localized to the left from the main peak (Fig. 3A, PS^+/PI^- vs. PI^+).

On the other hand, a DEX effect was noticed only after 60 min showing firstly peak broadening and subsequently a shift of the main peak after 90 min (Fig. 3B, DEX 60 vs. DEX 0). Volume changes were accompanied by the appearance of PS positive cells representing the region between the control and PI^+ cells (Fig. 3B, PS^+PI^-).

Thymocytes in the presence of curcumin continued shrinking during next 20 h showing FSC values only slightly higher than that observed in apoptotic cells after DEX stimulation (Fig. 3C, CUR/DEX 20 h vs. DEX 20 h).

3.4. Analysis of permeability to PI and plasma membrane asymmetry

CUR, regardless of DEX presence, caused an increase in membrane permeability to PI, showing a significantly increased fraction of the cells with compromised plasma membrane (PI^{bright}) compared to non-treated cells (Fig. 4A, CUR or CUR/DEX vs. CON, $P<0.05$). However, the amount of PI^{bright} cells after CUR coadministration did not exceed 7% during the first 2.5 h, while DEX alone made them 3% (Fig. 4A, CUR/DEX vs. DEX, $P<0.05$).

The subpopulation of PI^{dim} thymocytes corresponds to the cells with effective transport systems that prevent PI from reaching DNA despite a partly lost membrane integrity. These cells are commonly considered early apoptotic cells. Their number tended to increase only after DEX stimulation (Fig. 4A, DEX).

We analyzed phosphatidylserine exposure using Anx VI instead of the commonly used Anx V. The relative mass of Anx VI is 68 kDa, while that of Anx V is 33–37 kDa; Anx VI has eight binding sites for PS, while Anx V has only four (reviewed in [23,24]). This would make Anx VI a less sensitive probe in PS detection, but the stoichiometric 1:2 complex of Anx VI:FITC should compensate for the disadvantages men-

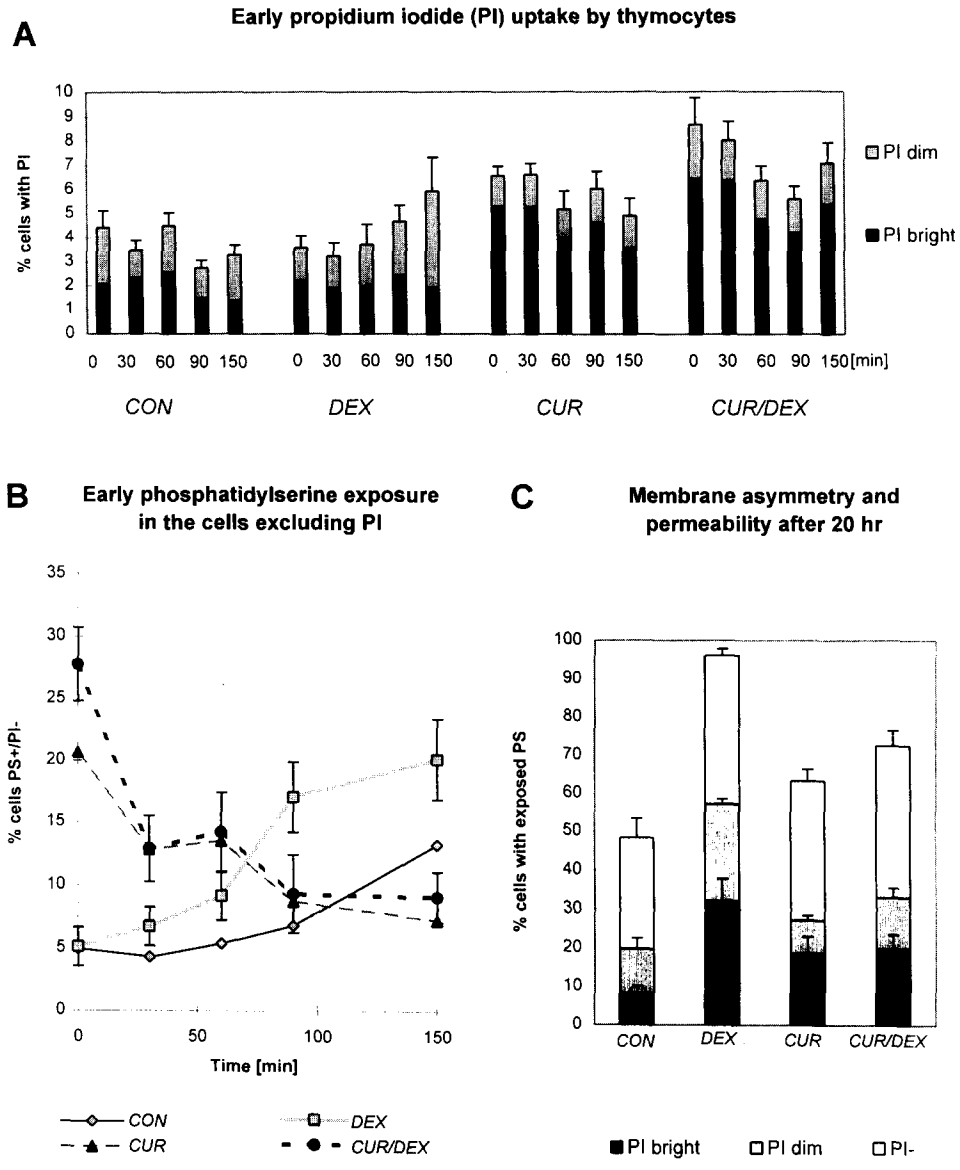

Fig. 4. Changes in plasma membrane permeability and asymmetry in thymocytes incubated for the indicated time at 37°C with dexamethasone (10^{-7} M; DEX) and/or curcumin (50 μM; CUR); CON, control, non-treated cells. A and C: Supravital PI staining (PI, 5 μg/ml) distinguishes PI^{bright} and PI^{dim} cells among PI positive cells (see Section 2). Percentages of PI^{bright} and PI^{dim} cells in population are expressed as means ± S.D. of five independent experiments and are significantly different at $P < 0.05$ for A: PI^{bright}-CON vs. CUR, DEX vs. CUR/DEX (0–150 min); PI^{dim}-DEX vs. CUR/DEX (at 150 min), and for C: PI^{bright}-CON vs. DEX, CON vs. CUR; PI^{dim}-CON vs. DEX, DEX vs. CUR/DEX (after 20 h). B and D: Double staining with Anx VI-FITC (1 μg/ml) and PI (1 μg/ml) distinguishes PS positive thymocytes among the cells excluding PI^- (see Section 2). % PS^+/PI^- per PI^- cells are presented as means of four separate experiments and are significantly different at $P < 0.05$ for B: DEX vs. CUR/DEX (0, 30, 90, 150 min), CON vs. CUR (0, 30, 60 min), CON vs. DEX (90, 150 min) and for D: CON vs. DEX and DEX vs. CUR/DEX (after 20 h).

tioned above. In any case, parallel experiments were performed with a commercial Anx V-FITC kit (Bender Med System, Vienna, Austria), and the results described below with Anx VI-FITC were fully confirmed (not shown). It is worth pointing out that porcine liver, as a source of annexin VI isolation, gives the opportunity to lower the costs of PS analysis. PS exposure was analyzed in the cells with intact membranes (i.e. PI^-) after electronic exclusion of thymocytes which were PI^+ (PI^{dim} and PI^{bright}). Curcumin induced an immediate increase in PS^+ cells either in thymocytes not treated with DEX or in DEX-treated ones (Fig. 4B, CUR and CUR/DEX vs. CON, $P < 0.05$). Such an extent of phospholipid scrambling was observed in DEX-stimulated cells only after 2.5 h (Fig. 4B, DEX vs. CON, $P < 0.05$). During the next 30 min in the presence of CUR, the amount of PS^+/PI^- cells dropped steeply and returned to control the value showing 9% until 1.5 h (Fig. 4B, CUR = CON). Compared to CUR, DEX led to slow PS redistribution observed to be significantly higher (20%, DEX) than control (9%, CON) after 1.5 h, at $P < 0.05$.

Fig. 4C shows that after 20 h incubation with DEX, 57% of cells were PI positive (32% PI^{bright}, 25% PI^{dim}). CUR coadministration significantly lowered that value to 33% (DEX vs. CUR/DEX, $P < 0.05$) which was not significantly different from the 26% due to CUR alone. In non-treated cells, 19% were PI positive.

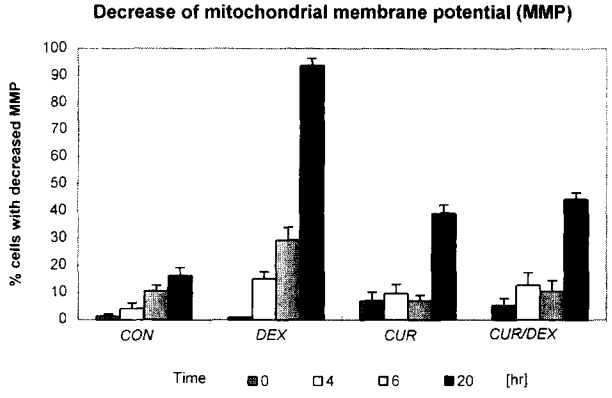

Fig. 5. Percentage of rat thymocytes with depolarized mitochondrial membrane, after incubation with curcumin (50 μM; CUR) and/or dexamethasone (10^{-7} M; DEX); CON, control, non-treated cells. Results are presented as means ± S.D. of four independent experiments. Data are significantly different at $P < 0.05$ at 4 h for CON vs. DEX, at 6 h for CON vs. DEX, DEX vs. CUR/DEX and after 20 h for all indicated treatments.

Prolonged DEX treatment led to PS exposure in 91% PI^- cells, as compared to 36% of non-treated cells (Fig. 4D, DEX vs. CON, $P < 0.05$). CUR coadministration significantly lowered the value to 59% (Fig. 4D, DEX vs. CUR/DEX, $P < 0.05$), not significantly different from the 50% of CUR alone.

3.5. *Measurement of mitochondrial membrane potential (Δ m)*

Curcumin induced an immediate decrease in $\Delta\psi_m$ in about 7% of the cells, regardless of DEX presence (Fig. 5, CUR or CUR/DEX). However, the number of cells with low $\Delta\psi_m$ did not exceed 13% during the next 6 h of CUR exposure in either DEX-treated or untreated cultures (Fig. 5, CUR; CUR/DEX). According to previous results [19] DEX caused a decrease in $\Delta\psi_m$ in about 30% of the thymocytes in about 6 h (Fig. 5, DEX).

A more prolonged incubation showed that CUR protected 50% of DEX-stimulated cells against $\Delta\psi_m$ collapse (Fig. 5, 44% cells depolarized in CUR/DEX vs. 94% after DEX, $P < 0.05$). However, CUR alone induced a significant mitochondrial membrane depolarization in 40% of the cells, while non-treated cells showed only 16% (Fig. 5, CUR vs. CON, $P < 0.05$).

4. Discussion

The physicochemical properties of curcumin such as hydrophobicity [25] predestine this molecule to easily pass the plasma membrane and spread throughout the lipid phase of membranous structures, i.e. endoplasmic reticulum (ER) and nuclear envelope. In this universal, non-specific way, curcumin could evoke structural and functional changes of cellular membranes simply partitioning into the lipid bilayer. Indeed, cells exposed to curcumin exhibited phosphatidylserine exposure, increased permeability of plasma membrane, decreased mitochondrial membrane potential and cell shrinkage. These features are commonly regarded as typically apoptotic. However, looking into the sequence of DEX-induced or CUR-evoked events, we found several differences. Cell shrinking was an early change in DEX-stimulated apoptosis, occurring within 1 h. During the next 30 min shrinking was followed by the exposure of phosphatidylserine. Then, cells continued shrinking, showing increased plasma membrane permeability after 2.5 h. Transport efficacy and plasma membrane integrity were still preserved there, thus preventing the entrance into the nucleus of a dye such as PI. Decrease in $\Delta\psi_m$ was noticed only after 4–6 h of incubation, and was predated by DNA fragmentation, which was evident 2 h earlier on agarose gel, and accompanied by the cytofluorimetric appearance of a hypodiploid peak (not shown), which is in agreement with previous observations [5,19]. On the other hand, curcumin caused cell shrinkage, PS exposure, increased permeability and $\Delta\psi_m$ collapse immediately after its addition and the extent of these changes during prolonged incubation was significantly lower than after DEX stimulation. In addition, nuclear morphology, lack of the hypodiploic fraction and of DNA fragmentation (not shown) suggested rather a protective effect of curcumin on DEX-treated rat thymocytes.

Loss of membrane integrity was observed in the presence of curcumin very early, which is in striking contrast to what occurs during the apoptotic program. In fact, rupture of plasma membrane usually occurs later, after the morphological changes in the nucleus and DNA fragmentation [26]. We could exclude the possibility of a necrotic type of cell death since microscopic examinations and flow cytometry analysis of cell morphology did not show uncontrolled swelling. We observed rather shrinking and protection against cell rupture (see also [5]). It was reported that lymphocytes, once stimulated to shrink, cannot reverse that process by regulatory volume increase and activate the apoptotic program ending with DNA fragmentation [27]. Although curcumin exposure resulted in a loss of cell volume, in contrast, there was no subdiploid peak or DNA laddering (see also [5]), which suggests distinct pathways leading to cell shrinkage or DNA fragmentation. Moreover, the inhibition of DNA endonuclease(s) observed in thymocytes seems to be indirect, since it is possible to induce DNA fragmentation in the presence of curcumin, as observed elsewhere [6].

We assume that PI uptake is the expression of a non-specific effect of the drug on the membrane structure. CUR partitioning into lipid bilayer could result in alterations of lipid packing or/and transbilayer motion of the lipids thus increasing the basal permeability of the plasma membrane. In erythrocytes, curcumin expanded the membrane (echinocytosis) and decreased the order of membrane lipids by inducing their rearrangement probably due to the appearance of non-bilayer structures during drug penetration (Jaruga et al., Exp. Cell Res., accepted). In thymocytes, adding curcumin also resulted in transient phosphatidylserine scrambling. Both membranous events, loss of asymmetry and increase of permeability, took place concomitantly and earlier than after DEX stimulation, suggesting the presence of an apoptosis-independent effect. Interestingly, the recovery of original PS location in such a short time could be possible only due to active aminophospholipid translocase, which was reported to be inhibited in the course of apoptosis [28–31]. Our observations in erythrocytes showed directly that curcumin did not affect flippase activity (Jaruga et al., Exp. Cell Res., accepted).

Curcumin was found to collapse $\Delta\psi_m$ immediately after its addition to cell cultures. Taking account of the lipophilic character of curcumin and its ability to dissociate protons (pK values for the three acid protons: 7.8, 8.5 and 9.0, respec-

tively [32]) curcumin might be suspected to increase permeability for protons and interfere with the energy-coupling system in the mitochondria, regardless of apoptosis induction. One could speculate that as a consequence of energy dissipation in mitochondria, cells are suffering from an increased level of reactive oxygen species. It was reported that coadministration of antioxidants like superoxide dismutase or catalase prevents curcumin-induced apoptosis in human leukemia cells [6]. On the other hand, curcumin is a known antioxidant and scavenger of free radicals [33]. It also increases the level of glutathione thus preventing thiol depletion occurring typically during apoptosis [34]. In view of this controversy, the role of curcumin in redox balance during apoptosis needs further study.

The membranous changes evoked by curcumin do not seem to depend on activation of the apoptotic program, although they could alter several biochemical pathways. For example, curcumin might modulate enzymes activities by e.g. changing the access to phosphatidylserine. It is tempting to speculate that inhibition of protein kinase C (PKC) by curcumin [9] is due to such an effect. Interestingly, the size of domains consisting of PS, MARCKS peptide, substrate and DAG increased proportionally to the PS concentration thus accelerating the PKC reaction [35]. Moreover, curcumin was found to inhibit PKC activity in a competitive way with regard to phosphatidylserine [9].

Curcumin has attracted the attention of many scientists since it is considered a potent anticancer drug. Searching for possible explanations of the basic mechanisms underlying a broad spectrum of its biological effects, we investigated the perturbations of membrane structures and/or activities which resulted from the localization of curcumin. Curcumin was found to affect structure and functions of cellular membranes and mimic typical events occurring during apoptosis. However, in striking contrast to what happens during apoptotic cell death, these events were immediate, partly reversible, and cells could recover in a relatively short time.

Finally, from a methodological point of view, it is worth pointing out that reliable discrimination of apoptosis in the presence of membrane-disturbing compounds like curcumin requires an accurate analysis of the meaning of the effects which are linked to the physicochemical properties of the drug rather than to its biological activities.

Acknowledgements: This work has been supported by KBN Grants 6 P04A 011 11 and 2224/4/91, FWPN grant 994/94, and grants from MURST and AIRC to C.F.

References

[1] Darzynkiewicz, Z. (1995) J. Cell. Biochem. 58, 151–159.
[2] Ammon, H.P.T., Safayhi, H., Mack, T. and Sabieraj, J. (1993) J. Ethnopharmacol. 38, 113–119.
[3] Stoner, G.D. and Mukhtar, H. (1995) J. Cell. Biochem. Suppl. 22, 169–180.
[4] Hanif, R., Qiao, L., Shiff, S.J. and Rigas, B. (1997) J. Lab. Clin. Med. 130, 576–584.
[5] Sikora, E., Bielak-Zmijewska, A., Piwocka, K., Skierski, J. and Radziszewska, E. (1997) Biochem. Pharmacol. 54, 899–907.
[6] Kuo, Min-Liang, Huang, Tze-Sing and Lin, Jen-Kun (1996) Biochim. Biophys. Acta 1317, 95–100.
[7] Huang, Mou-Tuan, Lysz, T., Ferraro, T., Abidi, T.F., Laskin, J.D. and Conney, A.H. (1991) Cancer Res. 51, 814–819.
[8] Rao, C.V., Rivenson, A., Simi, B. and Reddy, B.S. (1995) Cancer Res. 55, 259–266.
[9] Liu, J.-Y., Lin, S.-J. and Lin, J.-K. (1993) Carcinogenesis 14, 857–861.
[10] Tonnensen, H.H. and Greenhill, J.V. (1992) Int. J. Pharmaceut. 87, 79–87.
[11] Pulla Reddy, A.Ch. and Lokesh, B.R. (1994) Food Chem. Toxicol. 32, 279–283.
[12] Tonnensen, H.H., Arrieta, A.F. and Lerner, D. (1995) Pharmazie 50, 689–693.
[13] Smith, C.A., Gwyn, T.W., Kingston, R., Jenkinson, E.J. and Owen, J.J.T. (1989) Nature 337, 181–184.
[14] Bandorowicz, J., Pikuła, S. and Sobota, A. (1992) Biochim. Biophys. Acta 1150, 201–206.
[15] Vermes, I., Haanen, C., Steffens-Nakken, H. and Reutelingsperger, C. (1995) J. Immunol. Methods 184, 39–51.
[16] Darzynkiewicz, Z., Bruno, S., Del Bino, G., Gorczyca, W., Hotz, M.A., Lassota, P. and Traganos, F. (1992) Cytometry 13, 795–808.
[17] Cossarizza, A., Baccarani Contri, M., Kalashnikova, G. and Franceschi, C. (1993) Biochem. Biopys. Res. Commun. 197, 40–45.
[18] Salvioli, S., Ardizzoni, A., Franceschi, C. and Cossarizza, A. (1997) FEBS Lett. 411, 77–82.
[19] Cossarizza, A., Kalashnikova, G., Grassilli, E., Chiapelli, F., Salvioli, S., Capri, M., Barbieri, D., Troiano, L., Monti, D. and Franceschi, C. (1994) Exp. Cell Res. 214, 323–330.
[20] Cossarizza, A., Franceschi, C., Monti, D., Salvioli, S., Bellesia, E., Rivabene, R., Biondo, L., Rainaldi, G., Tinari, A. and Malorni, W. (1995) Exp. Cell Res. 220, 232–240.
[21] Polla, B.S., Kantengwa, S., François, D., Salvioli, S., Franceschi, C., Marsac, C. and Cossarizza, A. (1996) Proc. Natl. Acad. Sci. USA 93, 6458–6463.
[22] Nicoletti, I., Migliorati, G., Pagiacci, M.C., Grigniani, F. and Riccardi, C. (1991) J. Immunol. Methods 139, 271–279.
[23] Bandorowicz, J. and Pikula, S. (1993) Acta Biochim. Pol. 40, 281–293.
[24] Klee, C.B. (1988) Biochemistry 27, 6645–6653.
[25] Oetari, S., Sudibyo, M., Commandeur, J.N.M., Samhoedi, R. and Vermeulen, N.P.E. (1996) Biochem. Pharmacol. 51, 39–45.
[26] Ormerod, M.G., Sun, X.-M., Snowden, R.T., Davies, R., Fearnhead, H. and Cohen, G.M. (1993) Cytometry 14, 595–602.
[27] Bortner, C.D. and Cidlowski, J.A. (1996) Am. J. Physiol. 271 (Cell Physiol. 40), C950–C961.
[28] Fadok, V.A., Voelker, D.R., Campbell, P.A., Cohen, J.J., Bratton, D.L. and Henson, P.M. (1992) J. Immunol. 148, 2207–2216.
[29] Martin, S.J., Reutelingsperger, C.P.M., McGahan, A.J., Rader, J.A., van Schie, R.C.A.A., LaFace, D.M. and Green, D.R. (1995) J. Exp. Med. 182, 1545–1556.
[30] Verhoven, B., Schlegel, R.A. and Williamson, P. (1995) J. Exp. Med. 182, 1597–1601.
[31] Hampton, M.B., Vanags, D.M., Pörn-Ares, M.I. and Orrenius, S. (1996) FEBS Lett. 399, 277–282.
[32] Tonnensen, H.H. and Karlsen, J. (1985) Z. Lebensm. Unters. Forsch. 180, 402–404.
[33] Tonnensen, H.H. and Greenhill, J.V. (1992) Int. J. Pharmaceut. 87, 79–87.
[34] Jaruga, E., Bielak-Zmijewska, A., Sikora, E., Skierski, J., Radziszewska, E., Piwocka, K. and Bartosz, G. (1998) Biochem. Pharmacol. (in press).
[35] Yang, L. and Glaser, M. (1996) Biochemistry 35, 13966–13974.